Optimal ^{57}Co Flood Source Activity and Acquisition Time for Lymphoscintigraphy Localization Images

Martha V. Mar, Renee L. Dickinson, William D. Erwin, and Richard E. Wendt III

Division of Diagnostic Imaging, Department of Imaging Physics, University of Texas, M.D. Anderson Cancer Center, Houston, Texas

We evaluated different ^{57}Co flood source activities and acquisition times to obtain an optimal localization image for breast lymphoscintigraphy that would adequately outline the body and allow detection of nodes seen on the emission scan while minimizing unnecessary radiation exposure to the patient. **Methods:** An anthropomorphic thorax breast phantom representing an average-size patient was used to simulate nodes on a breast lymphoscintigraphy scan. The activities in the nodes at the time of acquisition ranged from 37 to 185 kBq (1–5 μCi). Four experiments were performed, consisting of 10-min emission and 3-min localization images. Anterior, posterior, and right and left lateral views of the thorax phantom were acquired, using each of 5 different ^{57}Co flood sources with activities ranging from 37 to 269 MBq (1.0–7.26 mCi). Ten 1-min localization images for each source were acquired and compared for quality. Three-minute localization images for 2 phantom thicknesses of 10 and 20 cm were acquired to determine the contrast-to-noise ratio for each ^{57}Co source. The total exposure was measured using an ion chamber survey meter. **Results:** All sources allowed visualization of the lymphatic nodes in acquisitions as short as 3 min. Images using the 126-MBq (3.41-mCi) source demonstrated an adequate body outline along with visualization of all nodes seen on the emission image. The 37-MBq (1.0-mCi) source did not provide sufficient definition of the body outline, whereas the hotter sources decreased node visualization by increasing the background around the nodes at the same time that they increased the patient exposure. Node activity of 37 kBq (1 μCi) became undetectable on the anterior localization images yet was still visible on the lateral image because of greater attenuation of ^{57}Co photons. The estimated dose rate from the ^{57}Co sheet sources was 0.641 μSv/MBq/h. **Conclusion:** Acquiring a 3-min localization scan using a 126-MBq (3.41-mCi) source provided the best combination of clear-body outline and visualization of all nodes seen on the emission image. The estimated dose to the patient from the 126-MBq (3.41-mCi) sheet source was very low (8.7 μSv for unilateral and 13.1 μSv for bilateral). Node detectability decreased in localization images acquired using ^{57}Co sources of higher activity. This effect would be more pronounced in lymphoscintigrams of thin patients compared with those of patients of average thickness.

Received Oct. 15, 2007; revision accepted Mar. 4, 2008.

For correspondence or reprints contact: Martha V. Mar, University of Texas, M.D. Anderson Cancer Center, 1515 Holcombe Blvd., Unit 1352, P.O. Box 83, Houston, TX 77030-1439.

E-mail: mmar@di.mdacc.tmc.edu

Key Words: breast; localization; lymphoscintigraphy; ^{57}Co flood source

J Nucl Med Technol 2008; 36:82–87
DOI: 10.2967/jnmt.107.047043

Several methods of outlining the body for lymphoscintigraphic localization imaging have been used clinically. One of the first methods used was simply outlining the boundaries of the patient's body with a handheld point source during the image acquisition (*1*). A similar but more complex method used a small amount of ^{99m}Tc activity in a syringe to perform a uniform sweep behind the patient (so-called activity-background painting) to simulate the transmission of sheet sources (*2*). Neither of these 2 methods is very practical because each is technically demanding and contributes to an increase of radiation exposure, but both are inexpensive. Another method of outlining the body contour is to acquire the image with 2 separate energy windows: one to detect primary photons from the ^{99m}Tc injection and the other to detect scattered ^{99m}Tc photons (*3*). A more advanced method is the use of a dual-head γ-camera equipped with ^{153}Gd–attenuation correction line sources, which can be used to generate an outline image (*1*). The line source is attached to one detector, and simultaneous ^{99m}Tc-emission and ^{153}Gd-planar localization images are acquired with the other detector. This technique can also be applied in the anterior or lateral projections or at other projection angles if needed. Currently, the most detailed localization images are SPECT/CT fusion images, which are superior to any patient outlining or backlighting technique because of the detailed, 3-dimensional anatomic localization capability (*4*). Although the methods discussed here have found limited acceptance for lymphoscintigraphy localization, the use of ^{57}Co flood source backlighting for lymphoscintigraphy imaging continues to be the most popular (*5,6*).

The popularity of the ^{57}Co backlighting method is most likely because of the ready availability of the ^{57}Co flood source; most clinical nuclear medicine departments use ^{57}Co sheet sources for daily quality-control testing and for collimator or extrinsic uniformity calibration for planar and

SPECT imaging. In facilities where more than 1 source is available, the question may arise as to which source activity would provide optimal localization imaging with the least amount of radiation exposure to the patient. The current study evaluated different source activities and image-acquisition times to improve lymphoscintigraphy localization imaging. The best imaging parameters were determined by ensuring that all lymph nodes visualized in the emission scan would also appear on the localization image while at the same time guaranteeing an adequate body outline to determine anatomic location. The dependence of the choice of best parameter on patient thickness was also evaluated.

Competing processes are at work when backlighting a lymphoscintigram with a ^{57}Co sheet source. Because the nodes themselves have a fixed activity, the more photons that penetrate the patient per unit time (a factor that depends directly on the ^{57}Co sheet source activity), the more likely the photons will mask the nodes in the image by reducing the node-to-background contrast. At the same time, a clear outline of the body requires a sufficient number of counts from the ^{57}Co source (where the number of counts necessary to adequately outline the body is reached by increasing the source activity or by increasing the acquisition time). The goal of this study was to find the sheet source activity and acquisition time for the ^{57}Co-backlighting image acquisition that offers the best compromise between body outline delineation and node detectability of a lymph node that is visualized in the planar emission scan.

MATERIALS AND METHODS

A modified anthropomorphic thorax breast phantom (Radiology Support Devices) representing an average-size (23-cm anteroposterior thickness) patient in combination with fillable spheres representing the injection site (4.0 mL) and lymph nodes (0.063 mL) was used to mimic 2 nodes on a breast lymphoscintigraphy scan (Figs. 1A and 1B).

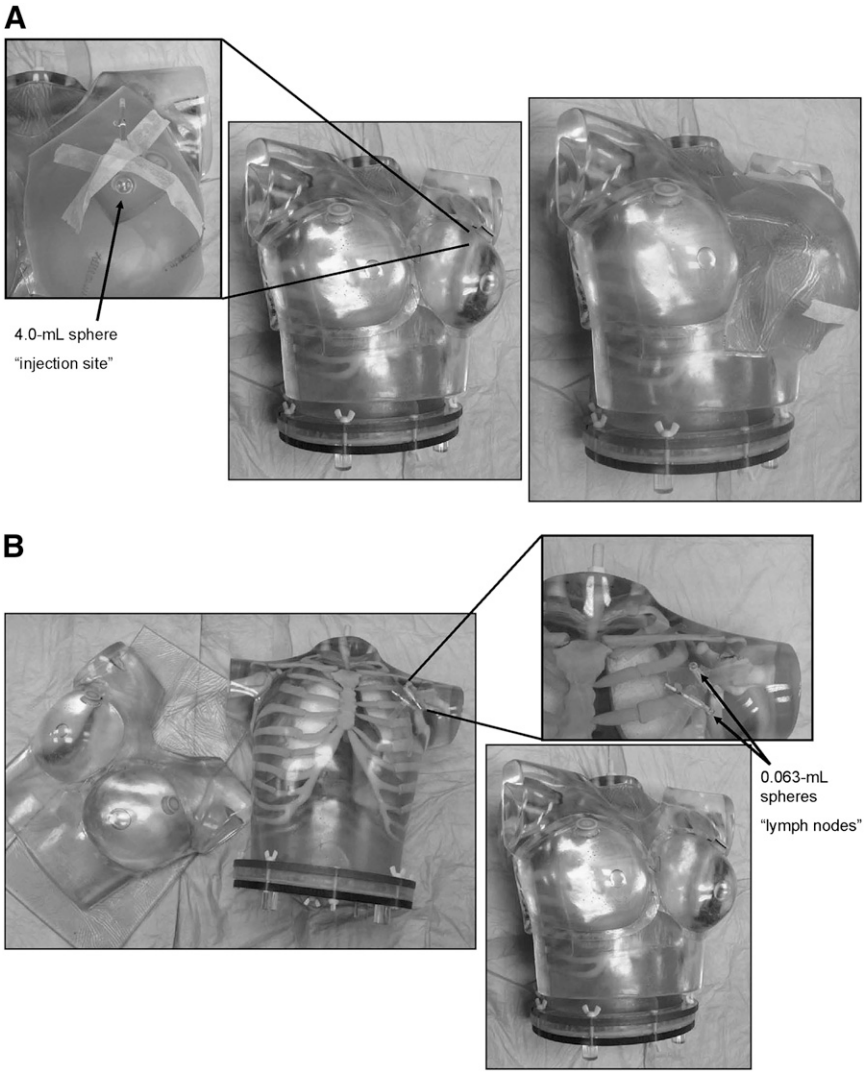

FIGURE 1. Modified anthropomorphic thorax breast phantom used to simulate breast lymphoscintigraphy injection-site uptake (A) and lymphatic drainage to 2 nodes (B).

The first of 4 experiments consisted of acquisitions of 10-min baseline emission images of the thorax phantom for all 4 common lymphoscintigraphic views: anterior, posterior, left lateral, and right lateral. Then, localization images for each of 5 different ^{57}Co flood sources with activities of 37, 126, 184, 220, and 269 MBq (1.0, 3.41, 4.96, 5.94, and 7.26 mCi) were acquired as a dynamic series of ten 1-min images. The individual 1-min dynamic images were summed to obtain 1-, 2-, 3-, 4-, 5-, 6-, 7-, 8-, 9-, and 10-min images. This collection of images with a range of count statistics was used to determine the shortest acquisition time that would yield adequate image quality.

After determining the shortest acquisition time for the transmission image, we conducted the second experiment, which consisted of 10-min emission and shortest acquisition-time localization images of anterior, posterior, and right and left lateral views of the thorax phantom, acquired with each of the 5 different ^{57}Co flood sources. These images were used to verify the detectability of nodes. The initial emission and dynamic localization images were acquired with an activity of 93 MBq (2.5 mCi) for the injection site, 185 kBq (5 μCi) for the spheric node, and 74 kBq (2 μCi) for the spheric node of ^{99m}Tc-pertechnetate. A second set of images used to verify node detectability using the optimal source activity was acquired with a lower activity of 56 MBq (1.5 mCi) for the injection site, 148 kBq (4 μCi) for the spheric node, and 37 kBq (1 μCi) for the spheric node of ^{99m}Tc-pertechnetate. The injection site and lymph node activities for the phantom were determined by a 200-patient retrospective chart review and are representative of the average activity range of ^{99m}Tc drainage to lymph nodes for breast lymphoscintigraphy studies (*7*). All images were acquired using low-energy, ultra-high-resolution collimators (256 × 256 matrix), with our standard clinical energy window used for imaging ^{99m}Tc: 15% width, centered on 140 keV.

Ideally the patient would attenuate all of the photons from the ^{57}Co sheet source. However, body sizes and hence transmission factors of patients vary, which necessitated an investigation of how the quality of the localization images would change given different anteroposterior and lateral thicknesses. Two nodes of approximately 37 and 148 kBq (1 and 4 μCi) were embedded into simulated adipose tissue (Superflab; Mick Radio-Nuclear Instruments, Inc.); different thicknesses of acrylic blocks (10 and 20 cm) were placed on the imaging couch with the Superflab and nodes on top. An additional acrylic block (5 cm thick) was placed over the nodes as a scatter medium. Three-minute localization images for the 2 block thicknesses of 10 and 20 cm were acquired for each ^{57}Co source, with the anterior collimator-to-node distance held constant. An identical region of interest (ROI) was drawn around each of the nodes and in the background. A contrast-to-noise ratio was calculated by taking the node ROI total counts, subtracting the total background counts in the identically sized background ROI, and dividing the results by the square root of the total background counts. This calculation was performed to ensure that the suggested source activity for lymphoscintigraphy was adequate for a wide range of patient sizes; the contrast-to-noise calculation was used to quantitatively assess whether a node would be visualized in an image with a known background activity.

Radiation-absorbed doses to the patient from each source were estimated on the basis of exposure measurements made with an ion chamber (Inovision 451B; Fluke) in rate mode. The meter was placed on top of the bed, with acrylic blocks surrounding the survey meter to simulate patient scatter. The ^{57}Co sources were placed one at a time on the face of the posterior detector, an arrangement similar to the one when scanning a patient, and the measured exposure rate for each sheet source was recorded (the μSv/h meter readings were assumed equivalent to effective dose rate, which is a conservative assumption). Lymphoscintigraphy studies require exposing the patient to ^{57}Co sheet sources for each of the views used to localize sentinel lymph nodes; the radiation absorbed for each individual view was calculated by multiplying each dose measurement by the time the patient would be exposed to the sheet source (3 min):

$$\text{Dose per view}\,[\mu\text{Sv}] = (\text{dose rate}) \times (\text{time per view})$$

$$\text{Dose per view}\,[\mu\text{Sv}] = (\mu\text{Sv/h}) \times (\text{h}).$$

The total estimated dose to the patient for a lymphatic study depends on whether the study is a bilateral or unilateral breast study; bilateral studies require 3 views for the transmission imaging (anterior, right lateral, and left lateral transmission images), whereas unilateral studies require only 2 views:

$$\text{Total dose}\,[\mu\text{Sv}] = (\text{dose per view}) \times (\text{number of views}).$$

RESULTS

The first experiment established the shortest acceptable localization acquisition time to be 3 min. All sources ranging from 37 to 269 MBq (1.0–7.26 mCi) allowed visualization of the lymphatic nodes with an acquisition time as short as 3 min (Figs. 2A–2D). The 1- and 2-min anterior localization images did not allow visualization of the 74-kBq (2-μCi) spheric node; however, the 74-kBq (2-μCi) spheric node was visible in the lateral image (Figs. 2C and 2D). The node was not visualized in the anterior image because of the higher background counts arising from transmission of the ^{57}Co backlighting photons through a smaller thickness of the simulated patient.

The second experiment used the shortest acquisition time from the first experiment to evaluate the source activity that would provide an adequate body outline while allowing visualization of all nodes seen on the emission scan. The 126-MBq (3.41-mCi) ^{57}Co sheet source provided the best compromise between clarity of the body outline and visualization of the weakest nodes (Figs. 2C and 2D). The 37-MBq (1.0-mCi) source did not provide a sufficiently distinct body outline, whereas the hotter sources increased the transmitted background counts around the nodes, thereby decreasing the contrast to the point of masking the node within the background.

After we determined an adequate source activity for body outline and node detectability, we acquired a 10-min emission image and 3-min localization image at that source activity with a lower activity of 56 MBq (1.5 mCi) in the injection-site sphere, a 148-kBq (4 μCi) spheric node, and a 37-kBq (1-μCi) spheric node. Node activities of 37 kBq (1 μCi) were undetectable on the anterior transmission

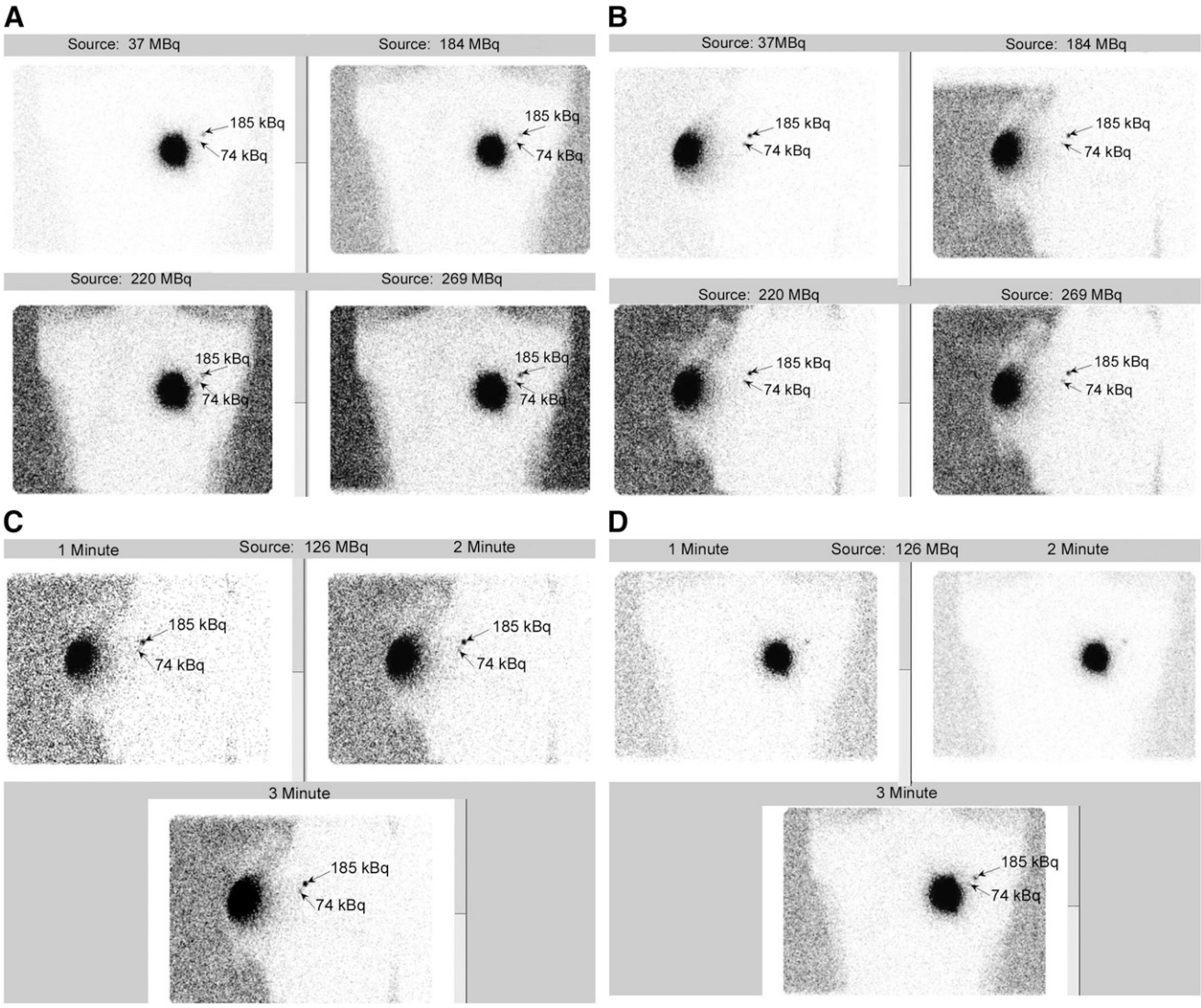

FIGURE 2. Different ^{57}Co sources (activities of 37, 126, 184, 220, and 269 MBq) allowed visualization of both nodes with acquisition time of 3 min (A–D). Anterior localization images (1 and 2 min) did not show both nodes; however, both nodes were visible on lateral images (C and D).

images yet were still visible on the lateral image because of the greater attenuation of the transmitted ^{57}Co photons in that orientation (Fig. 3). The lateral localization image (34-cm lateral phantom thickness) shows lower-activity nodes because of increased attenuation of ^{57}Co photons by more tissue; the reduction in counted ^{57}Co photons reduces the background, which increases the contrast and increases node detectability. The anterior view (23-cm anteroposterior phantom thickness) has less attenuation of photons than the lateral view because the photons have less tissue to traverse (*2*). The contrast in the anterior view is lower than that in the lateral view because of an increase of transmitted ^{57}Co photons detected within the outline of the patient, which increases the background and thus decreases the visualization of low-activity nodes (as was the case with the second spheric node with an activity of 37 kBq).

The third test was performed to ensure that the selected source activity would work both for average-size and thin patients. Table 1 and Figure 4 demonstrate the effect of attenuation of the ^{57}Co photons between 10- and 20-cm body thicknesses, indicating that node detectability on localization images will decrease with thinner patients, depending on the ^{57}Co activity.

The last experiment compared the estimated effective dose to the patient for the 5 different source activities available. Linear regressions of estimated effective dose versus ^{57}Co sheet source activity for unilateral and bilateral protocols yielded the functions $y = 0.1x - 0.4$ and $y = 0.1x - 0.5$, respectively. The calculated estimate of dose rate was 0.641 μSv/MBq/h. The best source activity for imaging 126 MBq (3.41 mCi) exposes patients to 8.7 μSv for total unilateral studies and 13.1 μSv for total bilateral

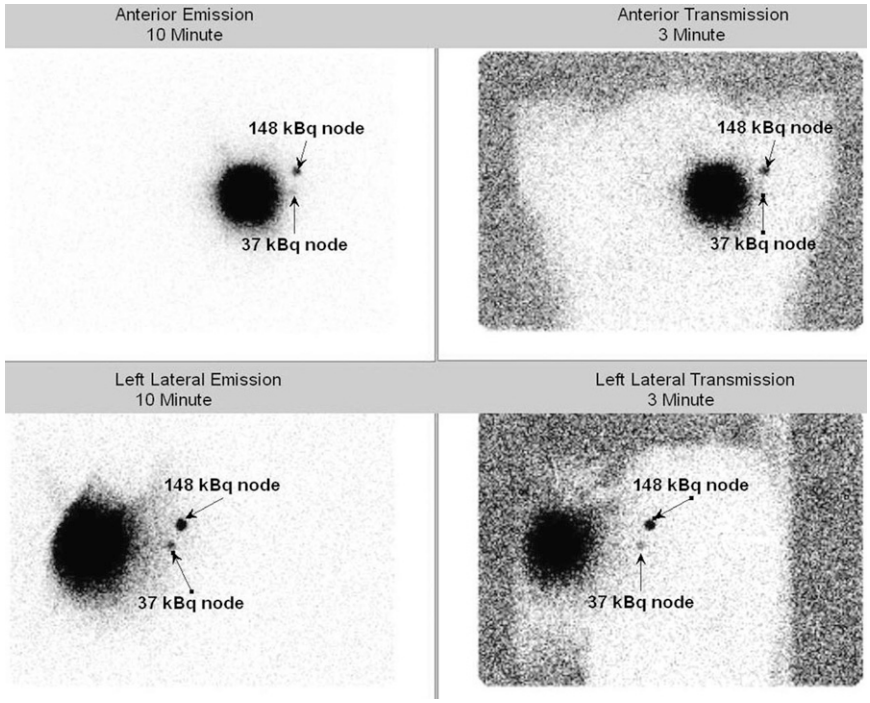

FIGURE 3. Node activities of 37 kBq were undetectable on anterior transmission images; however, they were visible on lateral transmission images using 126-MBq (3.41-mCi) ^{57}Co flood source.

studies (Table 2). Any additional single views would add approximately 4.4 μSv each to the patient's absorbed dose.

DISCUSSION

Technologists should be informed about the competing processes occurring during the acquisition of lymphoscintigram transmission imaging to provide the best images. In addition, technologists should be aware that when the source activity is less than the minimum activity for adequate delineation of the body outline, it is possible to improve the image quality by increasing the acquisition time proportionally. Consequently, the study time will be lengthened while the radiation exposure to the patient would be at best equivalent, and possibly greater. Hotter sources provide acceptable body outline with decreased scan time for the localization image, but the nodes may not be visualized because of a decreased node-to-background ratio. As the node activity decreases below 37 kBq (1 μCi), the node is masked in the localization image acquired with a higher activity source because a higher number of ^{57}Co photons penetrate through the patient and are counted, creating a higher background, and the same number of counts are detected from the node. Hotter sources increase the patient and technologists' radiation exposure during acquisition and setup time.

TABLE 1
CNR Calculations for 2 Block Thicknesses: 10 cm (Thin Patient) and 20 cm (Average Patient)

^{57}Co source activity (MBq)	Node 1 (total counts)	Node 2 (total counts)	Background (mean counts)	No. of pixels in background ROI	CNR node 1	CNR node 2
10-cm-thick acrylic						
37	169	505	0.52	27	41.4	131.0
126	158	514	0.89	27	27.3	100.0
184	176	537	1.15	27	26.0	90.8
220	185	582	2.00	27	17.8	71.9
269	213	550	2.48	27	17.8	59.0
20-cm-thick acrylic						
37	139	469	0.35	25	44.0	155.6
126	153	442	0.42	25	44.0	133.2
184	156	471	0.62	25	35.7	115.7
220	178	480	0.81	25	35.1	102.2
269	133	483	0.85	25	24.2	100.2

CNR = contrast-to-noise ratio.
Node detectability for transmission imaging decreases with thinner patients.

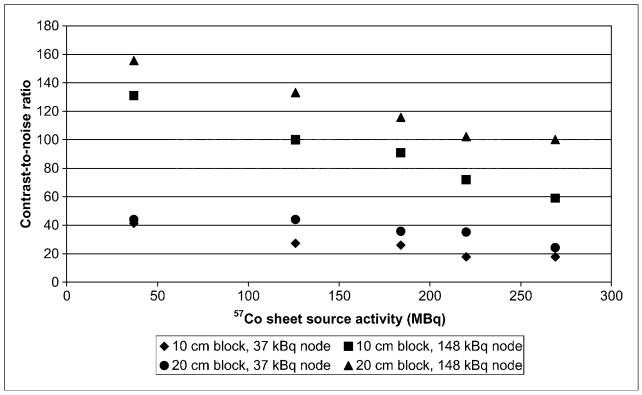

FIGURE 4. Plot of contrast-to-noise ratio versus source activity and block thickness for 2 node strengths.

The source activity used for transmission imaging is also affected by the various patient thicknesses. The results from the study using the 10- and 20-cm blocks showed that the contrast-to-noise ratio is higher for 20-cm than for 10-cm thicknesses because the body causes greater source photon attenuation at 20-cm thicknesses during localization imaging. Using high-activity sources will more significantly mask the nodes during transmission imaging in thin patients than in average patients. This is because of a greater number of ^{57}Co photons penetrating through less body, creating more background counts that mask the nodes. If one has a choice of 2 sources, using the lower activity for thin patients is recommended because thin patients will be the most affected because of the higher number of ^{57}Co photons penetrating through the patient and creating a higher background that will mask the node.

The objective of transmission scans is to see lymph nodes on the localization image that appear on the emission scan with sufficient body outline to determine the anatomic location, whereas the purpose of the emission scan is node detectability. Nonvisualization of lymph nodes during planar emission imaging occurs when the lymph nodes are close to the injection site or if they are located too deep within the patient. Several authors describe the use of SPECT/CT as an additional tool for inconclusive and unusual lymphoscintigram cases but do not eliminate the use of planar lymphoscintigraphy imaging for initial preoperative lymphatic mapping (*4,8,9*).

TABLE 2
Effective Dose Estimates for ^{57}Co Source Activities Given Standard 3-Minute Transmission Scans

^{57}Co source activity (MBq)	Measured exposure rate (μSv/h)	Exposure for single view (μSv)	Total for unilateral study (μSv)	Total for bilateral study (μSv)
37	20	1.00	2.0	3.0
126	87	4.35	8.7	13.1
184	113	5.65	11.3	17.0
220	145	7.25	14.5	21.8
269	178	8.90	17.8	26.7

CONCLUSION

Acquiring a 3-min localization image using a 126-MBq (3.41-mCi) source produced an adequate body outline while allowing visualization of all nodes seen on the emission image. These results suggest that the best source activity should be greater than 37 MBq (1.0 mCi) but not greater than 185 MBq (5.0 mCi). Node detectability decreased on localization images when using hotter ^{57}Co sources. This effect would be more pronounced in thin (10 cm) than in average patients. The estimated dose to the patient for 126 MBq (3.41 mCi) was acceptable (8.7 μSv for unilateral and 13.1 μSv for bilateral examinations) and can be estimated for any activity sheet source from the results in Table 2 (i.e., an average expected dose rate is 0.641 μSv/MBq/h).

Typically, flood sources used for nuclear medicine quality-assurance testing and calibration range from 185 to 555 MBq (5–15 mCi). Institutions that routinely dispose of ^{57}Co sheet sources that have decayed below 185 MBq (5 mCi) should consider keeping a decayed source for 1 extra replacement cycle (typically 9–12 mo), so that they would have a source of less than 185 MBq (5 mCi) to use for backlighting lymphoscintigrams. This is important for clinics that currently have only a single sheet source that is used both for γ-camera quality control and for backlighting for localization in lymphoscintigraphy. The results of this study suggest that both functions cannot be performed optimally with the same sheet source. Facilities that have more than 1 sheet source available should avoid using sources stronger than 185 MBq (5 mCi) for ^{57}Co backlighting.

REFERENCES

1. Clarke E, Notghi A, Harding K. Improved body-outline imaging technique for localization of sentinel lymph nodes in breast surgery. *J Nucl Med.* 2002;43:1181–1183.
2. Krynyckyi BR, Kim CK, Goyenechea M, Machac J. Methods to outline the patient during lymphoscintigraphy. *J Nucl Med.* 2003;44:992–993.
3. Fujii H, Yamashita H, Nakahara T, et al. Outlining the body contours with scattered photons in lymphoscintigraphy for sentinel nodes. *Ann Nucl Med.* 2000;14:401–404.
4. Even-Sapir E, Lerman H, Lievshitz G, et al. Lymphoscintigraphy for sentinel node mapping using a hybrid SPECT/CT system. *J Nucl Med.* 2003;44:1413–1420.
5. Scarsbrook AF, Ganeshan A, Bradley KM. Pearls and pitfalls of radionuclide imaging of the lymphatic system. Part 1: sentinel node lymphoscintigraphy in malignant melanoma. *Br J Radiol.* 2007;80:132–139.
6. Rossi CR, De Salvo GL, Trifiro G, et al. The impact of lymphoscintigraphy technique on the outcome of sentinel node biopsy in 1,313 patients with cutaneous melanoma: an Italian multicentric study (SOLISM-IMI). *J Nucl Med.* 2006;47:234–241.
7. Dickinson RL. *Technical Improvement of Lymphoscintigraphy* [master's thesis]. Houston, TX: University of Texas Health Science Center at Houston Graduate School of Biomedical Sciences; December 2007.
8. van der Ploeg IMC, Valdes Olmos RA, Nieweg OE, Rutgers EJTh, Kroon BBR, Hoefnagel CA. The additional value of SPECT/CT in lymphatic mapping in breast cancer and melanoma. *J Nucl Med.* 2007;48:1756–1760.
9. Lerman H, Lievshitz G, Zak O, Metser U, Schneebaum S, Even-Sapir E. Improved sentinel node identification by SPECT/CT in overweight patients with breast cancer. *J Nucl Med.* 2007;48:201–206.